Properties of flash roasted products from low-grade refractory iron tailings and improvement method for their magnetic separation index

He Wan [1,2], Xianlu Lu [1], Saija Luukkanen [2], Juanping Qu [2], Chonghui Zhang [1], Yanxin Chen [1], Xianzhong Bu [1]

[1] School of Resources Engineering, Xi'an University of Architecture and Technology, Xi'an 710055, China

[2] Oulu Mining School, University of Oulu, Oulu, FI-90014, Finland

Corresponding authors: wanhe@xauat.edu.cn (He Wan), buxianzhong@xauat.edu.cn (Xianzhong Bu)

Abstract: The properties of flash-roasted products from low-grade refractory iron tailings (IGRIT) and the improved method for their magnetic separation index were investigated by the MLA, XRD, iron phase analysis, and magnetic separation test. The results show the siderite and hematite in the IGRIT have been converted to magnetic iron after the flash roasting treatment with a time of 3-5 s; magnetic iron in roasted products has a monomeric dissociation of 37.20%, and a 75−100% exposed area of contiguous bodies as rich intergrowth was 29.83%, and that a 32.97 poor intergrowth; moreover, magnetic iron is mainly associated with muscovite and quartz. It is also found that the regrinding-magnetic separation (1500 Oe) treatment of the middling was beneficial to obtain more qualified iron concentrate products. Therefore, roasted products magnetic separation process in the absence/presence of the middling regrinding-magnetic separation treatment obtains an iron concentrate with 60.10%/ 60.12% iron grade and 72.04%/81.13% iron recovery. The iron concentrate from the magnetic separation process with middling regrinding-magnetic separation can have a 9% higher recovery than the process without middling regrinding-magnetic separation. The work is significant for helping to improve the utilization of IGRIT.

Keywords: roasted products, low-grade refractory iron tailings, magnetic separation, MLA

1. Introduction

Iron ore is an important resource for social construction and economic development (Zhang et al., 2022). In recent years, China's iron ore import rate is as high as 80% (Huang et al., 2020). Shortage of iron ore resources has become a major bottleneck restricting China's iron and steel industry and economic and social development (Xu and Dong, 2013). Therefore, maximizing the use of China's own iron ore resources is the key to mitigating the shortage of iron ore resources in China.

The resources of iron ore are abundant in China (Mishra and Swain, 2020). However, more than 97% of the iron ore is low-grade refractory iron ore (LGRIO) resources, such as limonite, siderite, and high phosphorus oolitic hematite (Roy et al., 2020; Yu et al., 2020). They are not effectively utilized due to the limitations of mineral processing technology and costs (Sun et al., 2020; Sun et al., 2019).

In recent years, magnetization roasting technology has attracted a lot of attention in the field of utilization of LGRIO (Sun et al., 2019; Das and Rath, 2020; Das et al., 2018). It can convert weakly magnetic minerals into strongly magnetic minerals and thus improving the separability of LGRIO (Sun et al., 2020; Yu et al., 2017). Moreover, several economical and effective roasting technologies for LGRIO have emerged, such as flash roasting, low-temperature roasting, and so on (Boehm et al., 2014; Wan et al., 2022; Pinto et al., 2022; Tang et al., 2019). However, studies on the nature of roasted products and the dissociation and magnetic separation of fine, complex, and highly disseminated types of iron ore have seldom been reported.

Some studies have found that coarser particle size is helpful in the magnetic separation of magnetic iron from gangue minerals (Yu et al., 2016; Guo et al., 2020). However, coarser particle size also means more intergrowth, which can easily lead to poor quality of the magnetic separation product. Therefore,

the process flow of stage grinding and separation are often used to improve the quality of iron concentrate. Guo et al. also found that particle size also significantly affects the magnetic separation of magnetic iron (Guo et al., 2020; Wang et al., 2018). As the magnetic particles gradually reduce in size, the magnetic induction intensity of the magnetic iron decreases. This will result in a gradual reduction in the magnetic induction intensity difference between fine magnetic iron and coarse-grained rich intergrowth, causing an increase in the challenge of their separation (Yuan et al., 2022). Therefore, it is necessary to further optimize the magnetic separation parameters based on the properties of roasted products to improve the magnetic separation index of LGRIO.

In response to the above problems, this paper investigated the process mineralogy properties of the flash-roasted product with a roasting time of 3-5s, analyzed the influence of the process parameters of middling product regrinding-magnetic separation on the Iron concentrate quality and recovery, and finally recommended the optimized magnetic separation process for the flash roasted product.

2.   Materials and methods

2.1. Materials

LGRIT in this work are from Daxigou Mining Company in Shangluo, China. Firstly, the LGRIT were ground to 90.0% −75 µm using a dry vertical mill. Secondly, powder products were reduced for 3-4 s at 780 °C with 10% CO in the CO_2 using a fluidized bed. Finally, powder products before and after roasting were used as sample for chemical multi-element analysis, XRD diffraction analysis, iron phase analysis and magnetic separation.

The results of the chemical multi-element analysis, XRD diffraction analysis and iron phase analysis of the LGRIT are shown in Fig. 1, Fig. 2 and Table 1. The results of Fig. 1 and Fig. 2 show that the total Fe content in the LGRIT was 20.25%; the major iron minerals in the iron tailing include siderite, hematite, and magnetite; the major gangue minerals in the LGRIT include quartz, muscovite, and kaolinite. Table 1 shows the content of Fe in carbonate/ hematite/ magnetic iron/ silicate is 12.85%/ 5.28%/ 1.60%/ 0.85%; the distribution rate of Fe in carbonate/ hematite/ magnetic iron/ silicate is 62.44%/ 25.66%/ 7.77%/ 4.13%.
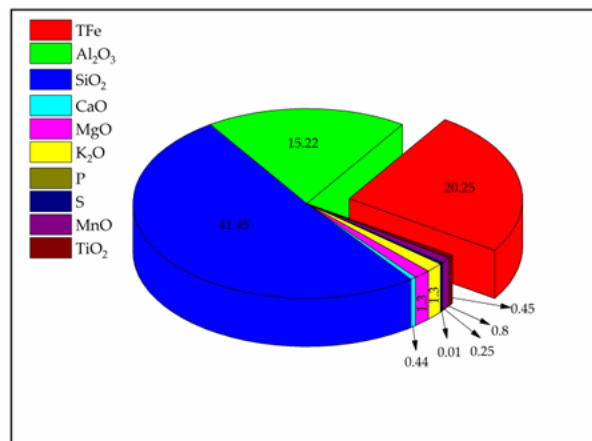

Fig. 1. The results of chemical multi-element analysis of the LGRIT

Table 1. Iron distribution in LGRIT

Fe Phase	In Carbonate	In Hematite	In Magnetic Iron	In Silicate	TFe
Content (%)	12.85	5.28	1.60	0.85	20.58
Distribution rate (%)	62.44	25.66	7.77	4.13	100.00

2.2. MLA analysis

MLA analysis was conducted by MLA software with SEM-EDS. During MLA work, different phases/minerals/ mineralogical parameters were distinguished/ identified/analyzed by the differences in the grey scale of backscattered electron images/ energy spectra/ modern image analysis
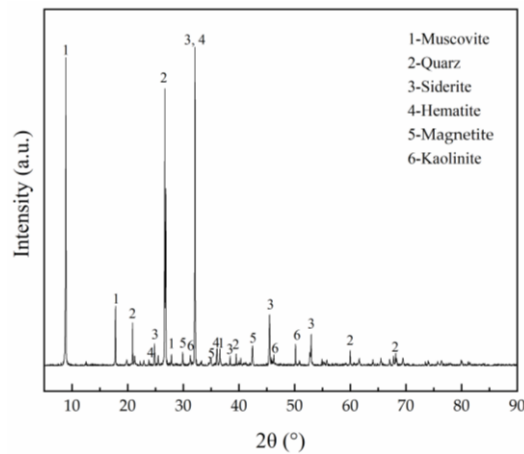
Fig. 2. The results of XRD diffraction analysis of the LGRIT

techniques (Sandmann, 2013; Schulz et al., 2019). Then, the data (element distribution, particle size distribution, liberation degree, intergrowth relationship, etc) of the LGRIT will be obtained.

2.3. Iron phase analysis

The iron phase analysis was used to analyze/obtain the content/ distribution rate of Fe in carbonate/ hematite/ magnetic iron/ silicate. In the process of iron phase analysis, the ore is first divided into magnetic part and non-magnetic part by magnetic separation (900 Oe) . The magnetic iron content can be obtained in the magnetic part, the non-magnetic part is treated with 2 mol/L acetic acid to dissolve the siderite, and the residue is leached with 4 mol/L hydrochloric acid containing 3% stannous chloride to extract hematite, pyrite is leached with aqua regia and the residue is iron-bearing silicate. The process of iron phase analysis was shown in Fig. 3 (Wan et al., 2022; Zhang et al., 2021).
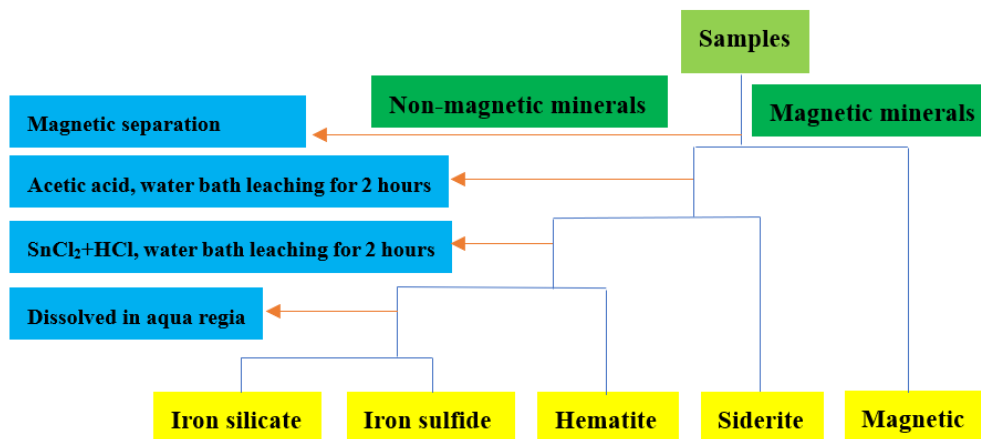

Fig. 3. Iron phase analysis

2.4. Magnetic separation

The roasted products (-74 μm 90%) were prepared into a 30% concentration pulp, then fed into a wet magnetic separator (DCXJ-400 × 240, Shandong Huatech Magnetics Technology Co., Weifang, China) with 1500 Oe, one rougher concentrate, and one tailing. The rougher concentrate was ground to 94.5% −38 μm using a wet ball mill (XMQ-240 × 90, Jilin Prospecting Machinery Factory, Jilin, China). The mill product was subjected to three sequential magnetic separations in the magnetic separator with 1300 Oe, 1000 Oe, and 700 Oe, and obtained one iron concentrate and three middlings. The schematic diagram of magnetic separation process is shown in Fig. 4.

The last two middlings from the process of the processing plant were combined and ground to 96.0% −38 μm using a wet ball mill (RK/ZQM-150 × 50, Wuhan Rock Grinding Equipment

Manufacturing Co., Wuhan, China). The mill product was subjected to 1-time magnetic separations in the magnetic separator with 1500 Oe and obtained one iron concentrate and one middling. The schematic diagram of the middling regrinding-magnetic separation is shown in Fig. 5.
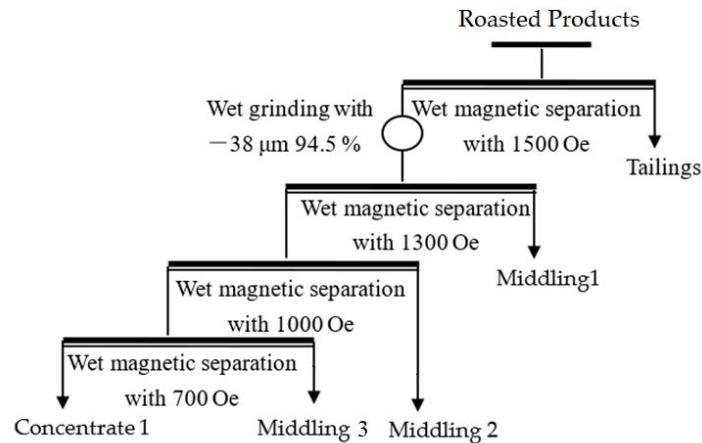

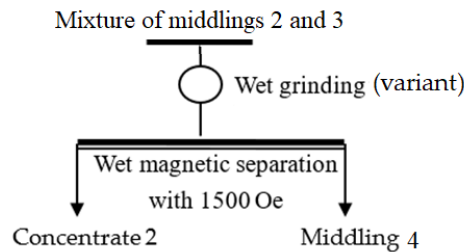Fig. 4. The flowchart of the magnetic separation of roasted products in the processing plant

Fig. 5. The flowchart of the middling regrinding-magnetic separation

3.   Results and discussion

3.1.   Properties of roasted products

3.1.1. Component of roasted products

The results of chemical multi-element analysis and iron phase analysis of the roasted products are shown in Fig. 6 and Table 2. The results of Fig .6 show that the total Fe content in the roasted products was 22.70%; compared to the LGRIT before roasting, the total Fe content in the roasted product increased by about 2.5%. Table 2 shows the content of Fe in carbonate/ hematite/ magnetic iron/ silicate is 0.12%/ 0.16%/ 21.88%/ 1.24%; the distribution rate of Fe in carbonate/ hematite/ magnetic iron/ silicate is 0.51%/ 0.68%/ 93.50%/ 5.30%. This indicates that the siderite and hematite in the LGRIT have been converted to magnetic iron after the flash roasting treatment (Fig. 7). Moreover, the maximum recovery of iron in the roasted product is not higher than 93.50%.

Table 2. Iron distribution in the roasted products

Fe Phase	In Carbonate	In Hematite	In Magnetic Iron	In Silicate	TFe
Content (%)	0.12	0.16	21.88	1.24	23.40
Distribution rate (%)	0.51	0.68	93.50	5.30	100.00

3.1.2. Particle size distribution of the siderite in the LGRIT before and after roasting

The particle size distribution of the siderite in the LGRIT before and after roasting from the MLA analysis are shown in Fig. 8.

The results of Fig. 8 show that the content of -38 μm particle size of the siderite in the LGRIT before roasting is less than that of the siderite in the LGRIT after roasting; the content of -4.1 μm particle size
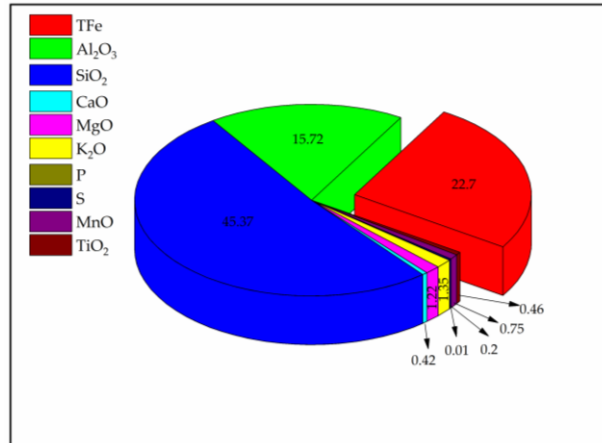
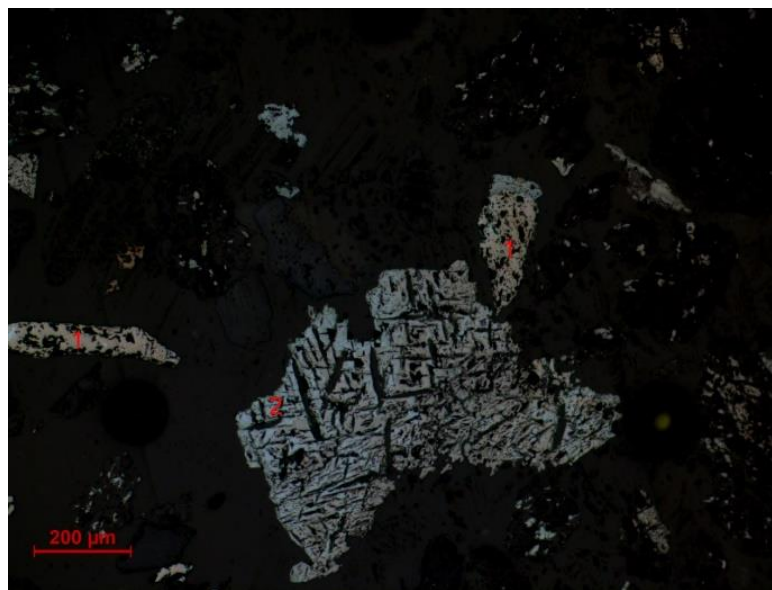Fig. 6. The results of chemical multi-element analysis of the roasted products

Fig. 7. Magnetic hematite mineralization of siderite and hematite
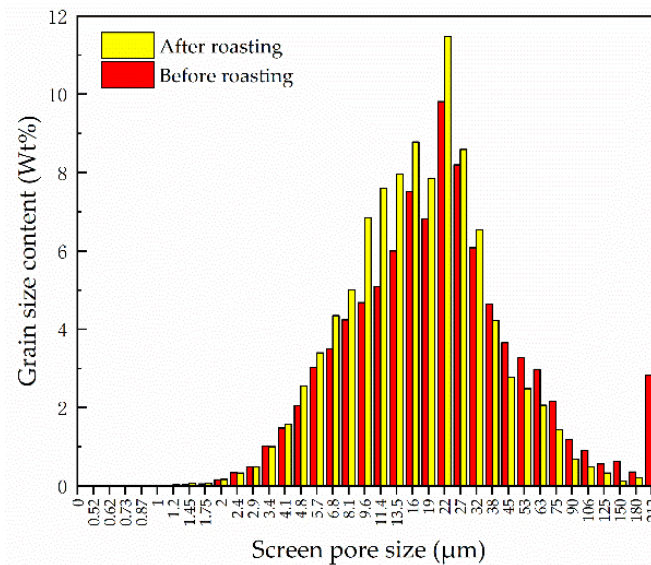1-Structure of siderite，2- Structure of hematite

Fig. 8. The particle size distribution of siderite in the LGRIT before and after roasting

of siderite in LGRIT is almost constant before and after roasting. This indicates that the roasting process could cause further dissociation of the +38 μm siderite. This result may be attributed to the decomposition reaction of siderite in a high-temperature environment and the release of carbon dioxide gas (García et al., 2020; Zhang et al., 2021). The decomposition reaction of siderite equations is as follows.

$$FeCO_3 \text{ (s)} \rightarrow FeO \text{ (s)} + CO_2 \text{ (g)} \tag{1}$$

3.1.3. Liberation degree and intergrowth characteristics of magnetic iron in the roasted products

The liberation degree characteristics of siderite/ magnetic iron (from siderite) in the LGRIT / roasted products are shown in Fig. 9. Fig. 9 shows that the siderite/ magnetic iron in the LGRIT / roasted products has a monomeric dissociation of 27.94%/ 37.20% and a 75−100% exposed area of contiguous bodies as rich intergrowth was 26.50%/ 29.83%. The total content of rich intergrowth and monomer siderite/ magnetic iron was 54.44%/67.03%. The content of poor intergrowth of siderite/ magnetic iron was over 45.56%/32.97. The poor intergrowth of magnetic iron (from siderite) in the roasted products is 12.59% less than that of siderite in the LGRIT. This indicates that the roasting process can promote the further dissociation of siderite with vein minerals. This agrees with the results of the particle size distribution of siderite in the LGRIT before and after roasting (Fig. 5).
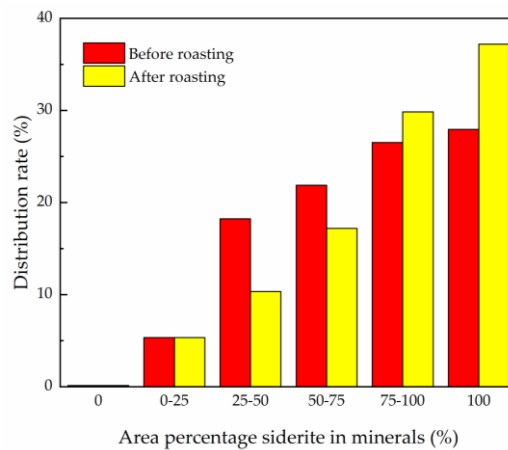

Fig. 9. Liberation degree characteristics of siderite/ magnetic iron in the LGRIT / roasted products

The intergrowth relationship between magnetic iron and major gangue minerals in the roasted products is shown in Fig. 10. The mineral map of the roasted products is shown in Fig. 11. Fig. 10 and 11 show that within the non-monolithic siderite mineral particles, the gangue minerals associated with siderite in the roasted products are quartz, muscovite, and kaolinite; moreover, as the exposure of siderite increases, the area occupied by the major gangue becomes gradually smaller; under the 0% and 0-25% exposed area of contiguous bodies, the major gangues are associated with siderite in the following order: quartz > muscovite > kaolinite; under the 25-50%,50-75% and 75-100% exposed area of contiguous bodies, the major gangues are associated with siderite in the following order: muscovite > quartz > kaolinite. These indicate that siderite in roasted products is mainly associated with muscovite and quartz. As a result, they may generate large amounts of middling products and result in a lower iron recovery.

3.2. Improving the magnetic separation index of roasted products

3.2.1. Magnetic separation index of roasted products based on the process of the processing plant

The flowchart of the magnetic separation of roasted products in the processing plant is shown in Fig. 4. The results are shown in Table 3. From the results in Table 3, we can find that the iron concentrate 1/middling 3/ middling 2/ middling 1 and tailings with Fe grade of 60.10%/ 38.47%/ 21.20%/ 9.44%/ 5.05% and iron recovery of 73.35%/ 8.16%/ 4.45%/ 5.07%/ 10.28% were obtained based on the

process of the processing plant; moreover, the iron content of both middling 2 and 3 is higher than 20%, especially, the iron content of middling 3 is nearly 40%. Therefore, the mixture of middling 2 and 3 will be considered for regrinding to further improve iron recovery.
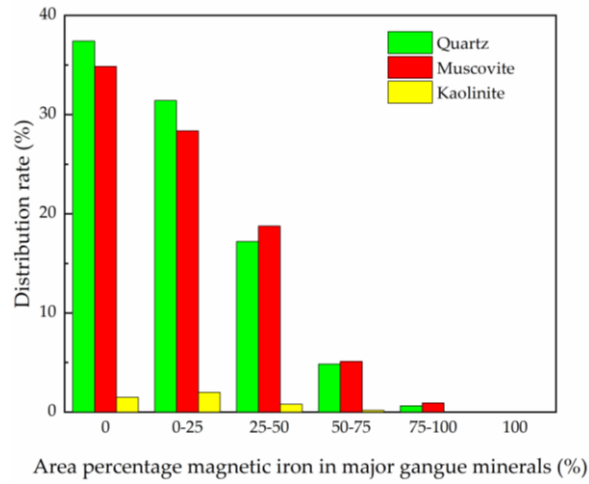

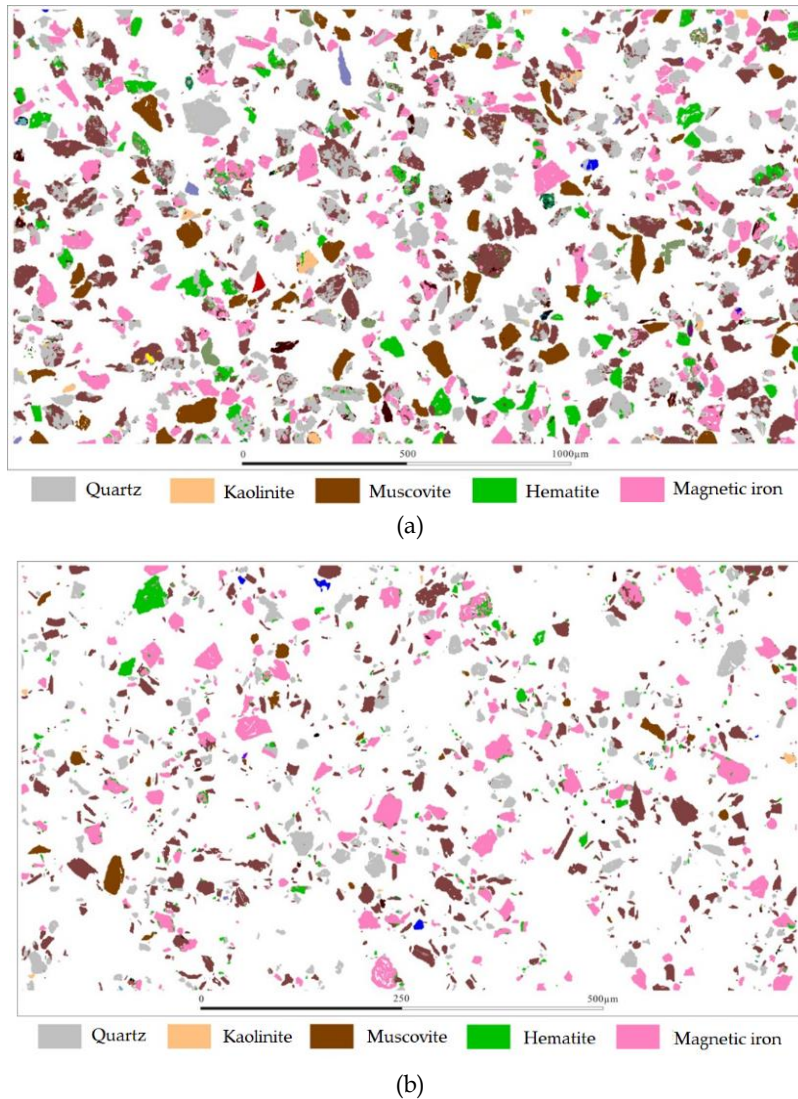Fig. 10. Intergrowth characteristics of siderite in the roasted products

(a)

(b)

Fig. 11. The mineral map of the roasted products.
(a) the particle size of −38~ +75 μm and (b) particle size of −38 μm

Table 3. The results of magnetic separation of roasted products based on the process of the processing plant

Name	Yield (%)	TFe (%)	
		Grade	Recovery
Concentrate 1	28.60	60.10	72.04
Middling 3	5.06	38.47	8.16
Middling 2	5.01	21.20	4.45
Middling1	12.82	9.44	5.07
Tailings	48.51	5.05	10.28
Roasted ore	100.00	23.86	100.00

3.2.2. Effect of middling regrinding on magnetic separation index

The flowchart of regrinding of the mixture of middling 2 and 3 is shown in Fig. 5. The results are shown in Fig.12. The results of Fig. 12 show that with the increase of regrinding fineness, the iron content curve in concentrate 2 tends to first increase and then flatten out, and the recovery always shows a decreasing trend. The iron content in concentrate 2 is higher than 60% and the recovery is 70.47% when the regrind fineness reaches 96% -38 μm. This indicates that the regrinding of the mixture of middle 2 and 3 is beneficial to obtain more qualified iron concentrate products. Therefore, a mixed iron concentrate can be obtained by mixing iron concentrates 1 and 2. The iron grade/recovery of the mixture of iron concentrate is 60.12%/81.13%.
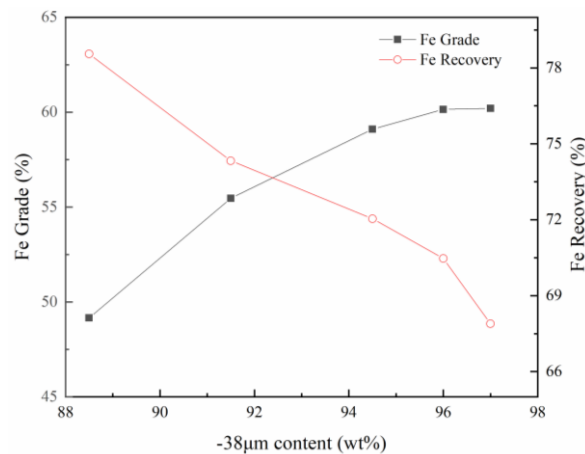

Fig. 12. The results of regrinding of the mixture of middling 2 and 3

3.2.3. Effect of magnetic field strength on the magnetic separation of the middling product

The flowchart of the effect of magnetic field strength on the magnetic separation of the middling product is shown in Fig. 5, in which regrinding fineness is -38μm 96.0%, and the magnetic field intensity is variant. The results are shown in Fig. 13. From Fig. 13, it can be seen that with the increase of magnetic field strength, the iron grade and recovery curve in iron concentrate 2 always show an increasing trend. This indicates that after regrinding in the middling, the magnetic iron particle size decreases, which causes its magnetic induction intensity to become weaker. Therefore, the high magnetic field strength is beneficial to the effective recovery of magnetic iron in fine particle size. This result is in agreement with the result of Guo et al. (2020).

3.2.4. Product Analysis of Iron Concentrate

Results of the study on the properties of roasted products indicated that quartz, muscovite, and kaolinite are the main gangue minerals in roasted products, especially quartz and muscovite are closely associated with siderite. The product analysis of the mixture of iron concentrate was carried out by XRD and chemical multi-element analysis. The results of them are shown in Fig. 14 and Table 4. Combining the results of Table 4 and Fig. 14 found that the iron content in the mixed iron concentrate is up to the requirements of the processing plant (>60%). SiO_2 is the main impurity in the

mixed iron concentrate. It has a content of 6.82% and is derived from quartz and muscovite. The result is in agreement with the intergrowth relationship between magnetic iron and major gangue minerals in the roasted products (Fig. 10). The content of other impurities is rather low, e.g., S (0.14%), P (0.013%), Cu (0.092%), Pb (0.054%), Zn (0.018%), Sn (0.012%), As (0.006%) and F (<0.01). This indicates that the mixed iron concentrate reaches the first grade of C60 in the Chinese iron concentrate quality standard. Therefore, Fig. 15 is proposed as the optimized magnetic separation process for the flash-roasted product.
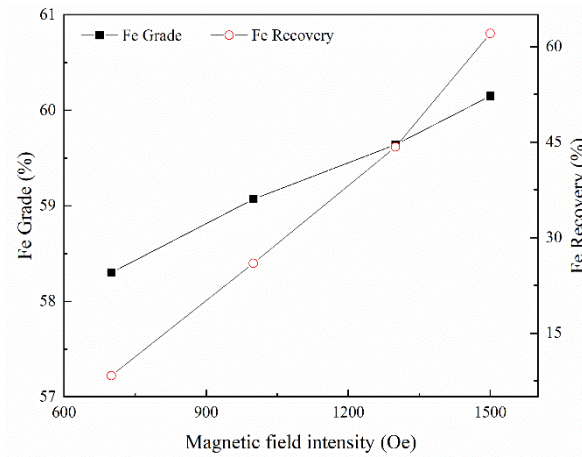

Fig. 13. Effect of magnetic field strength on the magnetic separation of the middling product
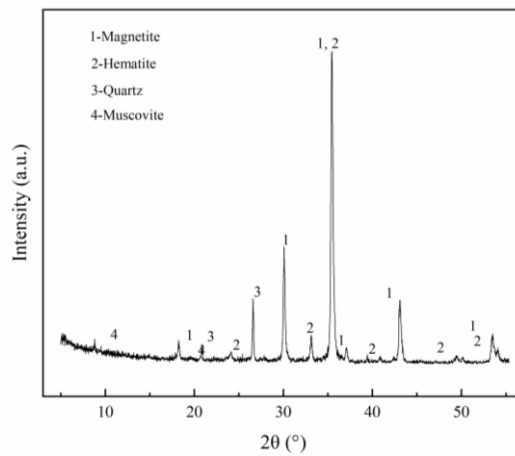

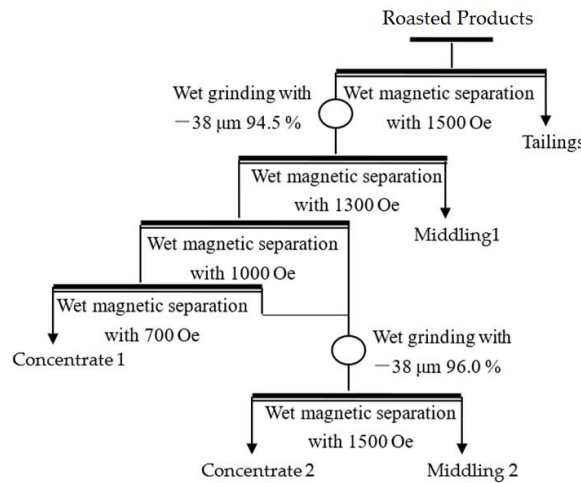Fig. 14. The result of XRD analysis of mixed iron concentrate

Fig. 15. the optimal process flow of magnetic separation for the flash-roasted product

Table 4. The result of chemical multi-element analysis of mixed iron concentrate

Element	TFe	SiO_2	S	P	Cu	Pb	Zn	Sn	As	F
Content (%)	60.12	6.82	0.14	0.013	0.092	0.054	0.018	0.012	0.006	<0.01

4. Conclusions

The properties of flash-roasted products from LGRIT and the enhancement method for their magnetic separation index were investigated. The results of the iron phase analysis show the distribution of iron in carbonate/ hematite/ magnetic iron accounted for 0.51%/ 0.68%/ 93.50% of the total iron content in the roasted product. This indicates that the siderite and hematite in the LGRIT have been converted to magnetic iron after the flash roasting treatment. The MLA results show that magnetic iron in roasted products has a monomeric dissociation of 37.20% and that a 75−100% exposed area of contiguous bodies as rich intergrowth was 29.83%, and a 32.97 poor intergrowth; moreover, magnetic iron is mainly associated with muscovite and quartz. Therefore, they may cause a decrease in the quality of iron concentrate. The results of middling regrinding and magnetic separation show that the regrinding of the mixture of middle 2 and 3 is beneficial to obtain more qualified iron concentrate products; after regrinding in the middling, the magnetic iron particle size decreases, which causes its magnetic induction intensity to become weaker. Therefore, the high magnetic field strength is beneficial to the effective recovery of magnetic iron in fine particle size. The product analysis of the mixture of iron concentrate found that the mixed iron concentrate reaches the first grade of C60 in the Chinese iron concentrate quality standard. The optimized magnetic separation process can be used to obtain a mixture of iron concentrate with 60.12%/81.13% iron grade/recovery. The optimized magnetic separation process has a 9% higher recovery than the magnetic separation process of the processing plant.

Acknowledgments

References

BOEHM, A., BOEHM, M., KOGELBAUER, A., 2014. *Neutrons for mineral processing–thermo diffractometry to investigate mineral selective magnetizing flash roasting*. Chemie Ingenieur Technik, 86(6), 883-890.

DAS, B., RATH, S. S., 2020. *Existing and new processes for beneficiation of Indian iron ores.* Transactions of the Indian Institute of Metals, 73(3), 505-514.

DAS, S. K., PRASAD, R., SINGH, R. P., 2018. *Characterisation-Assisted Reduction Roasting of BHJ, West Singhbhum, Jharkhand, India.* Transactions of the Indian Institute of Metals, 71(6), 1357-1362.

GARCÍA, A. C., LATIFI, M., CHAOUKI, J., 2020. Kinetics of calcination of natural carbonate minerals. Minerals Engineering, 150, 106279.

GUO, X., REN, W., ZHANG, M., DAI, S., ZHAO, T., ZHU, J., 2020. *Effects of grinding fineness on magnetism and agglomeration of magnetite.* Journal of Central South University: (Science and Technology), 2020, 51(9): 2373-2378. (in Chinese)

HUANG, J., LIU, J., ZHANG, H., GUO, Y., 2020. *Sustainable risk analysis of China's overseas investment in iron ore.* Resources Policy, 68, 101771.

MISHRA, D.P.; SWAIN, S.K., 2020. *Global trends in reserves, production and utilization of iron ore and its sustainability with special emphasis to India*. J. Mines Met. Fuels, 68, 11–18.

PINTO, P. S., MILAGRE, L. E., MOREIRA, L., ROCHA JUNIOR, H. P., SALVIANO, A. B., ARDISSON, J. D., LAGO, R. M., 2022. *Iron Recovery from Iron Ore Tailings by Direct Hydrogen Reduction at Low Temperature and Magnetic Separation*. Journal of the Brazilian Chemical Society, 33, 969-977.

ROY, S.K., NAYAK, D. RATH, S.S., 2020. *A review on the enrichment of iron values of low-grade Iron ore resources using reduction roasting-magnetic separation*. Powder Technol. 367, 796–808.

SANDMANN, D., 2013. *Use of mineral liberation analysis (MLA) in the characterization of lithium-bearing micas*. J. Miner. Mater. Character. Eng. 1, 285.

SCHULZ, B., MERKER, G., GUTZMER, J., 2019. *Automated SEM mineral liberation analysis (MLA) with generically labelled EDX spectra in the mineral processing of rare earth element ores*. Minerals, 9, 527.

SUN, Y., ZHANG, X., HAN, Y., LI, Y., 2020. *A new approach for recovering iron from iron ore tailings using suspension magnetization roasting: A pilot-scale study*. Powder Technol. 361, 571–580.

SUN, Y., ZHU, X., HAN, Y., LI, Y., 2019. *Green magnetization roasting technology for refractory iron ore using siderite as a reductant*. J. Clean. Prod. 206, 40–50.

TANG, Z. D., GAO, P., HAN, Y. X., GUO, W., 2019. *Fluidized bed roasting technology in iron ores dressing in China: A review on equipment development and application prospect.* Journal of Mining and Metallurgy B: Metallurgy, 55(3), 295-303.

WAN, H., YI, P., LUUKKANEN, S., QU, J., ZHANG, C., YANG, S., BU, X., 2022. *Recovering Iron Concentrate from Low-Grade Siderite Tailings Based on the Process Mineralogy Characteristics*. Minerals, 12(6), 676.

WANG, S., GUO, K., QI, S., LU, L., 2018. *Effect of frictional grinding on ore characteristics and selectivity of magnetic separation*. Mine. Eng., 122: 251-257.

XU, F., DONG, Y. X., 2013. *China's global strategy of mineral resources under the background of the financial crisis*. Applied Mechanics and Materials, 295, 2696-2700.

YU, J. W., HAN, Y. X., LI, Y. J., GAO, P., 2016. *Effect of magnetic pulse pretreatment on grindability of a magnetite ore and its implication on magnetic separation*. Journal of Central South University, 23(12), 3108-3114.

YU, J., HAN, Y., LI, Y., GAO, P., 2020. *Recent advances in magnetization roasting of refractory iron ores: A technological review in the past decade.* Miner. Process. Extr. Metall. Rev. 41, 349–359.

YU, J., HAN, Y., LI, Y., GAO, P., 2017. *Beneficiation of an iron ore fines by magnetization roasting and magnetic separation.* International Journal of Mineral Processing, 168, 102-108.

YUAN, S., DING, H., WANG, R., ZHANG, Q., LI, Y., GAO, P., 2022. *The mechanism of suspension reduction on Fe enrichment with low-grade carbonate-containing iron ore.* Advanced Powder Technology, 33(7), 103643.

ZHENG, M., WU, P., YOU, B., 2022. *Economic security evaluation and early warning of iron ore resources in China.* Geological Bulletin of China, 41(5), 836-845.

ZHANG, Q., SUN, Y., HAN, Y., GAO, P., LI, Y., 2021. *Thermal Decomposition Kinetics of Siderite Ore during Magnetization Roasting*. Min. Metall. Explor. 38, 1497–1508.